Front. Phys. 13(2), 137403 (2018)
https://doi.org/10.1007/s11467-017-0739-x

RESEARCH ARTICLE

Analytical assessment of some characteristic ratios for s-wave superconductors

Ryszard Gonczarek[1], Mateusz Krzyzosiak[2,†], Adam Gonczarek[3], Lucjan Jacak[1]

[1] *Faculty of Fundamental Problems of Technology, Wrocław University of Technology, Wybrzeże Wyspiańskiego 27, 50-370 Wrocław, Poland*
[2] *University of Michigan–Shanghai Jiao Tong University Joint Institute, 800 Dongchuan Road, Shanghai 200240, China*
[3] *Faculty of Computer Science and Management, Wrocław University of Technology, Wybrzeże Wyspiańskiego 27, 50-370 Wrocław, Poland*
Corresponding author. E-mail: †m.krzyzosiak@sjtu.edu.cn
Received October 9, 2017; accepted November 16, 2017

We evaluate some thermodynamic quantities and characteristic ratios that describe low- and high-temperature s-wave superconducting systems. Based on a set of fundamental equations derived within the conformal transformation method, a simple model is proposed and studied analytically. After including a one-parameter class of fluctuations in the density of states, the mathematical structure of the s-wave superconducting gap, the free energy difference, and the specific heat difference is found and discussed in an analytic manner. Both the zero-temperature limit $T = 0$ and the subcritical temperature range $T \lesssim T_c$ are discussed using the method of successive approximations. The equation for the ratio $\mathcal{R}_1$, relating the zero-temperature energy gap and the critical temperature, is formulated and solved numerically for various values of the model parameter. Other thermodynamic quantities are analyzed, including a characteristic ratio $\mathcal{R}_2$, quantifying the dynamics of the specific heat jump at the critical temperature. It is shown that the obtained model results coincide with experimental data for low-T_c superconductors. The prospect of application of the presented model in studies of high-T_c superconductors and other superconducting systems of the new generation is also discussed.

Keywords superconductivity, characteristic ratios, fluctuation of the DoS

PACS numbers 74.25.Bt, 74.62.Yb

Frontiers of Physics

1 Introduction

Research in the field of superconductivity, which has entered its second century since the first observation of the phenomenon, is notably marked by a number of milestone events. These include the discovery of high-temperature superconducting ceramics in the 1980s, successful implementation of quantum information processing on superconducting qubits, and a more recent breakthrough brought by iron-based superconducting materials in 2008 [1]. That latter discovery has placed superconductivity in the forefront of condensed matter physics again and has resulted in an unprecedented outburst of research activity, with 15,000 papers on iron-based superconductors published over the period from 2008 to 2015 alone [2].

Many advanced technologies have been increasingly relying on novel solid-state materials, including high-T_c copper-oxide quasi-two-dimensional superconductors and various doped superconducting compounds such as spinel- and perovskite-type structures of superconducting compounds of a trivalent rare-earth and a divalent alkali-earth ion. Other classes of superconducting materials that have been actively studied and applied in recent years include superconducting compounds of MgB_2 with a C, Al, or Sc substitution and organic superconductors with a controlled bandwidth and band filling [3–12].

Ongoing studies on the origin and the mechanism of superconductivity in novel superconducting systems have been closely accompanied by efforts to theoretically describe and predict numerous phenomena and trends observed in experiments. An important tool for quantitative theoretical studies on superconducting systems is

the gap equation, along with the equation determining the carrier concentration, and the free energy. It appears in similar forms in BCS theory, the formalism of Eliashberg equations, and the Van Hove scenario, with the latter taking into account the low-dimensional structure of high-T_c materials. To evaluate the fundamental thermodynamic functions such as free energy, thermodynamic potential, entropy, heat capacity, and other quantitative parameters (including the transition temperature, energy gap values, heat capacity jump, critical current, critical magnetic field, isotope shift, *etc.*), one should analyze the gap equation together with the corresponding formulas for the concentration of superconducting carriers, thermodynamic potential, and critical magnetic field [3, 4, 13–19].

Theoretical studies, confirmed by experimental results, point to the fact that, by applying a high external pressure after the dissociation process in H_3S, a superconducting state is created with a transition temperature of 203 K [20–27]. A quantitative theoretical description of such superconducting systems requires taking into account spin fluctuations or strong-correlation effects. These can be included by means of an effective Hamiltonian of the strongly interacting Hubbard model with a given (multiband) one-particle dispersion relation enriched by self-energy corrections, fitted carrier concentration, and a quite general form of the pairing potential, with the latter usually decomposed into antisymmetric and symmetric parts, determining the symmetry of the order parameter [28–38].

In the present paper, we show that some of the above problems can be studied in a systematic manner using powerful analytical tools [5–8, 39], allowing us to derive, for the first time, some fundamental relations for crucial thermodynamic parameters characterizing a superconducting system. These include the energy gap, critical temperature, free energy, and heat capacity difference (at zero temperature or in the subcritical temperature range) as functions of a single fluctuation in the density of states characterized by a parameter χ. In particular, the following characteristics of superconducting systems can be studied: (i) the relation between the energy gap Δ at $T = 0$ and the transition temperature T_c, quantified by the ratio $\mathcal{R}_1 \equiv 2\Delta(0)/T_c$, and (ii) the characteristic ratio $\mathcal{R}_2 \equiv \Delta C(T_c)/C_N(T_c)$, where $\Delta C(T_c) = C_S(T_c) - C_N(T_c)$ defines the heat capacity jump between the superconducting and the normal phase at the transition temperature. Another ratio that we define and study in this paper, $\mathcal{R}_4 \equiv T_c d[\Delta C(T)/C_N(T_c)]/dT$, gives the slope of the line tangential to the reduced specific heat difference curve at the transition temperature. All these ratios can be derived and discussed as functions of the fluctuation-related parameter χ. Because we do not include any effects of the magnetic field in this paper, the discussion of another characteristic ratio, $\mathcal{R}_3 \equiv H_c(0)/\sqrt{\nu_0}\Delta(0)$, where $H_c(0)$ denotes the zero-temperature critical magnetic field, has been left aside for the time being.

For a standard BCS superconductor, the four ratios are equal to $\mathcal{R}_1 = 3.528$, $\mathcal{R}_2 = 1.426$, $\mathcal{R}_3 = 3.545$, and $\mathcal{R}_4 = 2.628$, respectively [16, 17, 40]. Moreover, the ratios $\mathcal{R}_1$, $\mathcal{R}_2$, and $\mathcal{R}_4$ can be measured by using experimental techniques and therefore are available for comparison with our theoretical results.

Finally, it worth emphasizing that, after inclusion of some pairing potential contributions, there may emerge phase transitions with a discontinuous order parameter and pseudogap regions [4, 41]. The results presented in this paper cannot be extrapolated to these cases.

2 Formalism and basic equations

In this paper, we use the conformal transformation method [39], which has been developed recently, to study various properties of strongly correlated electron systems [3, 6–8, 28, 42–44]. In the context of superconductivity studied within the Green's function formalism, the method is applied to a set of two fundamental equations in momentum space consistent with the mean-field approximation. The first is the gap equation,

$$\Delta_{\boldsymbol{k}} = \sum_{\boldsymbol{k}'} V(\boldsymbol{k},\boldsymbol{k}') \frac{\Delta_{\boldsymbol{k}'}}{E_{\boldsymbol{k}'}} \tanh \frac{E_{\boldsymbol{k}'}}{2T}, \tag{1}$$

where $E_{\boldsymbol{k}} = \sqrt{(\xi_{\boldsymbol{k}} - \mu)^2 + \Delta_{\boldsymbol{k}}^2}$. The gap equation (1) is supplemented by another self-consistent equation, namely, the equation for charge carrier concentration,

$$n = \frac{1}{N} \sum_{\boldsymbol{k}} \left(1 - \frac{\xi_{\boldsymbol{k}} - \mu}{2E_{\boldsymbol{k}}} \tanh \frac{E_{\boldsymbol{k}}}{2T} \right). \tag{2}$$

Equation (2) determines the chemical potential μ and allows one to express μ in Eq. (1) in terms of the conduction band filling n (defined for the normal phase at $T = 0$), with N denoting the number of lattice sites. The advantage of such a general approach is that it allows us to study superconducting systems with a partially filled conduction band as well. The transformed form of the dispersion relation, $\xi_{\boldsymbol{k}}$, is usually defined with respect to the Fermi level.

The approach, briefly outlined in the above paragraph, can be applied to anisotropic superconducting systems with an arbitrary dispersion relation for spin-singlet s-wave or d-wave symmetry states, as well as for the spin-triplet p-wave symmetry state. The role of other factors, such as the carrier concentration and the pairing potential amplitudes in the singlet and triplet channels,

V_0 and V_1, respectively, can be discussed in more complicated scenarios to comment on the stability of the singlet and the triplet symmetry states [3, 8, 35, 42, 43, 45, 46]. In this paper, however, we limit the discussion to spin-singlet s-wave superconducting systems with a single constant pairing potential amplitude g.

2.1 Gap equation and free energy

Let us consider anisotropic superconductors, with exactly the spin-singlet s-wave formed, and the carrier concentration and pairing potential amplitudes $V_0 = g$ and $V_1 = 0$ being fixed. If we assume the dispersion relation $\xi_{\mathbf{k}}$ as determined in the model under discussion, then, after applying the conformal transformation method developed in Refs. [3, 28, 43], the gap equation (1) can be transformed into the form

$$\frac{1}{g} = \nu_0 \left\langle \int_0^{\epsilon_p} \frac{\mathrm{d}\xi \mathcal{K}(\xi,\omega)}{2\sqrt{\xi^2+\Delta^2}} \tanh \frac{\sqrt{\xi^2+\Delta^2}}{2T} \right\rangle, \tag{3}$$

where ν_0 is the density of states of the BCS type and ξ_p is the so-called cutoff parameter. The cutoff parameter is unique to each possible pairing mechanism [39], and it corresponds to the Debye energy $k_{\mathrm{B}}T_{\mathrm{D}}$ for systems with electron–phonon pairing potential. The symbol $\langle \cdots \rangle$ denotes averaging over the polar (or the spherical) angle(s) ω in two-dimensional (or three-dimensional) space, respectively [28, 39]. Note that the dimensionless scalar field of the density of states, $\mathcal{K}(\xi,\omega)$, is the only function depending on ω in the equation. Therefore, after averaging over the angular coordinates, Eq. (3) reduces to the form

$$\frac{1}{g} = \nu_0 \int_0^{\epsilon_p} \frac{\mathrm{d}\xi \mathcal{N}(\xi)}{2\sqrt{\xi^2+\Delta^2}} \tanh \frac{\sqrt{\xi^2+\Delta^2}}{2T}, \tag{4}$$

where $\mathcal{N}(\xi) = \langle \mathcal{K}(\xi,\omega) \rangle$ is the dimensionless density of states. The density of states appears as the final product in the conformal transformation approach. As such, it can also include effects of particle–hole asymmetry and an extra factor, as, e.g., the spectral function defined in the Eliashberg equations. Because for the BCS model $\mathcal{N}(\xi) \equiv 1$, we assume it to be in the form $\mathcal{N}(\xi) = 1+\rho(\xi)$. According to previous studies [44], the function ρ can substantially change various parameters of a superconducting system, especially if the function has a narrow fluctuation (a peak) in the vicinity of the Fermi surface. Moreover, it turns out that results obtained for peaks of various shapes yield similar results. Therefore, at this point, we do not need to consider any particular analytical properties of the function ρ, treating it as a locally constant function.

In the next step, after introducing the symbols $x = \xi/(2T)$, $x_p = \xi_p/(2T)$, and $D = \Delta/(2T)$, we can rewrite Eq. (4) as

$$\frac{1}{g} = \nu_0 \int_0^{x_p} \frac{\mathrm{d}x[1+\varrho(x)]}{\sqrt{x^2+D^2}} \tanh\left(\sqrt{x^2+D^2}\right). \tag{5}$$

Here the function $\rho(\xi)$ has been redefined into $\varrho(x)$, which can be again modeled in various manners. The factor g can be eliminated by taking into account Eq. (5) in the limiting cases $T = T_{\mathrm{c}}$ and $D = 0$. Using relations given in Ref. [35] one can easily reproduce the free energy difference between the superconducting and normal phases, $\Delta F = F_{\mathrm{S}} - F_{\mathrm{N}}$, as follows:

$$\Delta F = \int_0^{\Delta} \mathrm{d}\Delta' \left\{ \frac{\Delta'}{g} - \nu_0 \int_0^{x_p} \mathrm{d}x \frac{[1+\varrho(x)]\Delta'}{\sqrt{x^2+[\Delta'/(2T)]^2}} \cdot \tanh\left(\sqrt{x^2+[\Delta'/(2T)]^2}\right) \right\}. \tag{6}$$

To apply the results to traditional and high-temperature s-wave superconductors, it is enough to take into account a model form of $\varrho(x)$, which so far has been treated as constant in local intervals. As we have already stated, the function $\varrho(x)$ should feature a narrow fluctuation (a peak) in the vicinity of the Fermi surface. Because various shapes of the fluctuation produce similar results, we propose to take the function $\varrho(x)$ in the following normalized form:

$$\varrho_j(x) = \chi \frac{(2j-1)!!}{2^{j-1}(j-1)!} \cosh^{-2j} x, \tag{7}$$

where $j = 1, 2, \ldots$. The fixed parameter χ denotes the height of the local fluctuation and, as such, it can be either positive or negative, with the latter case corresponding to the situation in which the averaged fluctuations away from the Fermi level are higher than those at the Fermi level. The parameter $\chi = 2\mathrm{arccosh}(\sqrt[2j]{2})$ denotes the half-width of the fluctuation. Note that, using $\varrho_j(x)$ in such a form, one can derive analytic forms of Eq. (5) by employing the relations given in Refs. [47, 48]. Moreover, for $j \to \infty$ the function $\varrho_j(x) \to 2\chi\delta(x)$, where $\delta(x)$ is the Dirac delta [47, 48], as illustrated in the bottom-right panel of Fig. 1.

The case $\chi = 0$ corresponds to the BCS model, *i.e.*, the free-electron model with a restricted pairing interaction near the Fermi surface, which is characterized by two independent parameters g and ξ_p whose values should be taken with reference to real superconductors. That will allow us to compare some thermodynamic quantities in the BCS model with the values obtained within the present approach.

2.2 Zero-temperature case

Considering the case of $T = 0$ and assuming $\varrho(x)$ in the form (7), we consequently redefine the symbols introduced in Eq. (5) as $x = \xi/(2T_c(\chi))$, $x_{p,\chi} = \xi_p/(2T_{\mathrm{c}}(\chi))$,

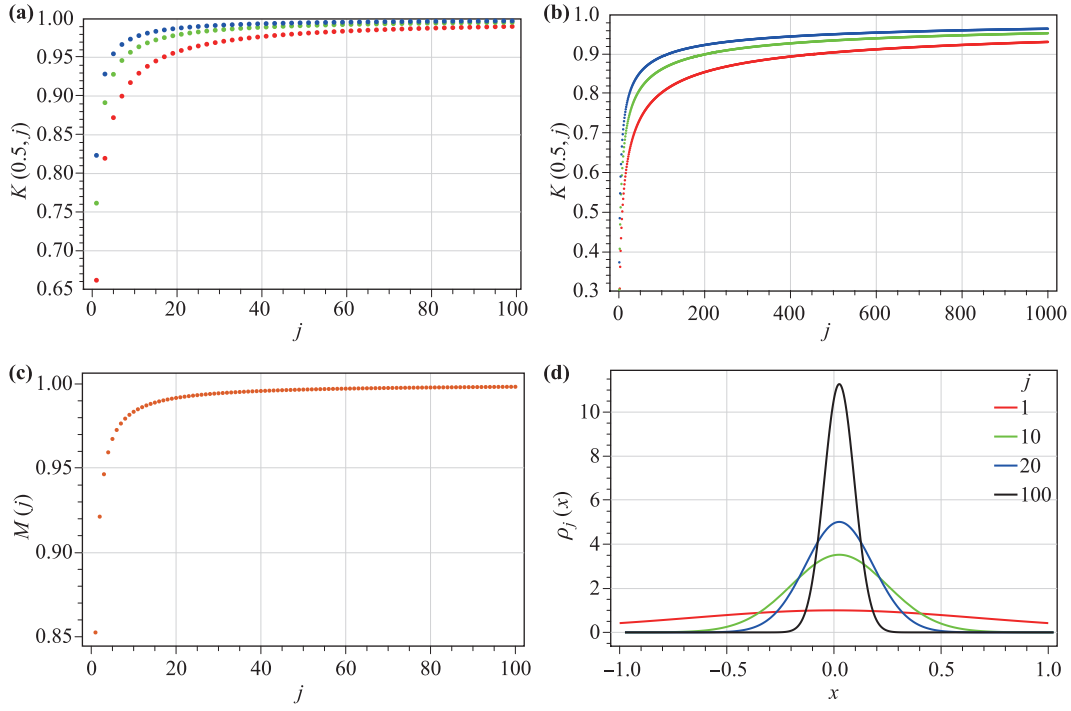

Fig. 1 Convergence tests for the integrals K **(a)** and L **(b)** with $D = 0.5$ (red), 0.75 (green), and 1.0 (blue), as well as for the integral M **(c)**. The local fluctuation assumes the shape of the Dirac delta for large values of j **(d)**.

and $D(0,\chi) = \Delta(0,\chi)/(2T_c(\chi))$. Then Eq. (5) assumes the form

$$\frac{1}{g} = \nu_0 \int_0^{x_{p,\chi}} \frac{\mathrm{d}x[1+\varrho_j(x)]}{\sqrt{x^2+D^2(0,\chi)}}. \tag{8}$$

Evaluating the integral, we obtain

$$\frac{1}{g\nu_0} = \ln\frac{\xi_p/T_c(\chi)}{D(0,\chi)} + \frac{\chi}{D(0,\chi)} K\left(D(0,\chi), j\right), \tag{9}$$

where

$$K(D,j) = \frac{(2j-1)!!}{2^{j-1}(j-1)!} D \int_0^\infty \frac{\mathrm{d}x}{\sqrt{x^2+D^2}} \cosh^{-2j} x,$$

and $D \in (0.5, 1)$ and hence $0.661 < K(D,j) < 1$, $K(D,100) > 0.990$, and $K(D,j) \to 1$ for $j \to \infty$ (see Fig. 1).

The free energy difference can be found using Eq. (6). After some algebra we get

$$\Delta F(0,\chi) = -\frac{\nu_0}{4}\Delta^2(0,\chi) - \nu_0\chi T_c(\chi)\Delta(0,\chi)L(D(0,\chi),j), \tag{10}$$

where

$$L(D,j) = \frac{(2j-1)!!}{2^{j-1}(j-1)!}\frac{2}{D}\int_0^\infty \mathrm{d}x \cdot \frac{x^2+\frac{1}{2}D^2 - x\sqrt{x^2+D^2}}{\sqrt{x^2+D^2}} \cosh^{-2j} x.$$

Note that $L(D,j)$ tends to 1 for $j \to \infty$ (see Fig. 1) and in this limit Eq. (10) assumes the form

$$\Delta F(0,\chi) = -\frac{\nu_0}{4}\Delta^2(0,\chi) - \nu_0\chi T_c(\chi)\Delta(0,\chi).$$

2.3 Critical temperature case

At the critical temperature $T = T_c(\chi)$, when $\Delta = 0$, Eq. (5) yields

$$\frac{1}{g\nu_0} = \ln\frac{\xi_p}{2T_c(\chi)} + \ln\frac{4\mathrm{e}^C}{\pi} + \chi M(j), \tag{11}$$

where $C = 0.577$ is the Euler constant. Moreover,

$$M(j) = \frac{(2j-1)!!}{2^{j-1}(j-1)!}\int_0^\infty \frac{\mathrm{d}x}{x}\tanh x \cosh^{-2j} x,$$

and $0.852 < M(p) < 1$, $M(20) = 0.992$, and $M(j) \to 1$ for $j \to \infty$ (see Fig. 1). According to the results presented in Refs. [47, 48], the function $M(j)$, where $j = 2, 3, \ldots$, can be found analytically. Namely, $M(j)$ can be transformed to the form

$$M(j) = \frac{(2j-1)!!}{2^{j-1}(j-1)!}\left[2jI_j - (2j+1)I_{j+1}\right],$$

where the integral

$$I_j = \int_0^\infty \ln x \cosh^{-2j} x \mathrm{d}x$$

can be evaluated analytically.

2.4 Relations between thermodynamic magnitudes

Let us assume that the same parameters ν_0, g, and ξ_p are simultaneously fixed for both the BCS model $\xi = 0$ and the developed approach $\xi \neq 0$. Then, from Eq. (9), one can obtain

$$\Delta(0,\chi) = \Delta(0,0)\exp\left[\frac{\chi}{D(0,\chi)}\,K\left(D(0,\xi),j\right)\right], \quad (12)$$

whereas from Eq. (11) one finds

$$T_{\rm c}(\chi) = T_{\rm c}(0)\exp[\chi M(j)], \quad (13)$$

which confirms that the critical temperature is modified by fluctuations of the density of states with respect to the BCS model. Namely, $T_{\rm c}$ decreases for negative values of χ and increases if χ is positive, exactly as occurs for high-$T_{\rm c}$ superconductors [39].

3 Characteristic ratios

3.1 Ratio $\mathcal{R}_1(\chi)$

Equations (9) and (11), derived in the previous sections, allow us to consider the ratio $\mathcal{R}_1 = 2\Delta(0)/T_{\rm c}$ as a function of χ, dependent on $K(D,j)$ and $M(j)$. Comparing the right sides of Eqs. (11) and (9), and taking into account that $\mathcal{R}_1(\chi) = 4D(0,\chi)$, we have

$$\mathcal{R}_1(\chi) = \mathcal{R}_1\exp\left\{\chi\left[\frac{4K(\frac{1}{4}\mathcal{R}_1(\chi),j)}{\mathcal{R}_1(\chi)} - M(j)\right]\right\}, \quad (14)$$

which in the limit $j \to \infty$ simplifies to the form

$$\mathcal{R}_1(\chi) = \mathcal{R}_1\exp\left\{\chi\left[\frac{4}{\mathcal{R}_1(\chi)} - 1\right]\right\}. \quad (15)$$

We find $\mathcal{R}_1(\chi)$ numerically, assuming that $0.3 \leqslant \mathcal{R}_1(\chi) \leqslant 10$ and including that, in the BCS case ($\chi = 0$), the value of the ratio is $\mathcal{R}_1 = 3.52$. The solutions of Eqs. (14) and (15) for various values of χ are presented in Fig. 2. The graphs in Fig. 2 show that the curve obtained for $j = 100$ is very close to that corresponding to $j \to \infty$. It is worth emphasizing at this point that, although the solution of Eqs. (14) and (15) has been formally found for a wide range of values of the parameter χ, one should keep in mind that this is the free energy that determines whether the superconducting phase is the stable phase for a given values of parameters. This problem will be discussed in detail in Section 3.2.3, where the range of values of the parameter χ will be determined.

Comparing the obtained results with the experimental data for some superconducting materials [14–18, 23, 49–51], we can map the values of the parameter χ onto specific superconducting systems. Table 1 includes a number of classical and high-temperature superconductors with their corresponding values of the parameter χ. Having found the value of χ for a given superconducting system, we can then use it to compute the values of

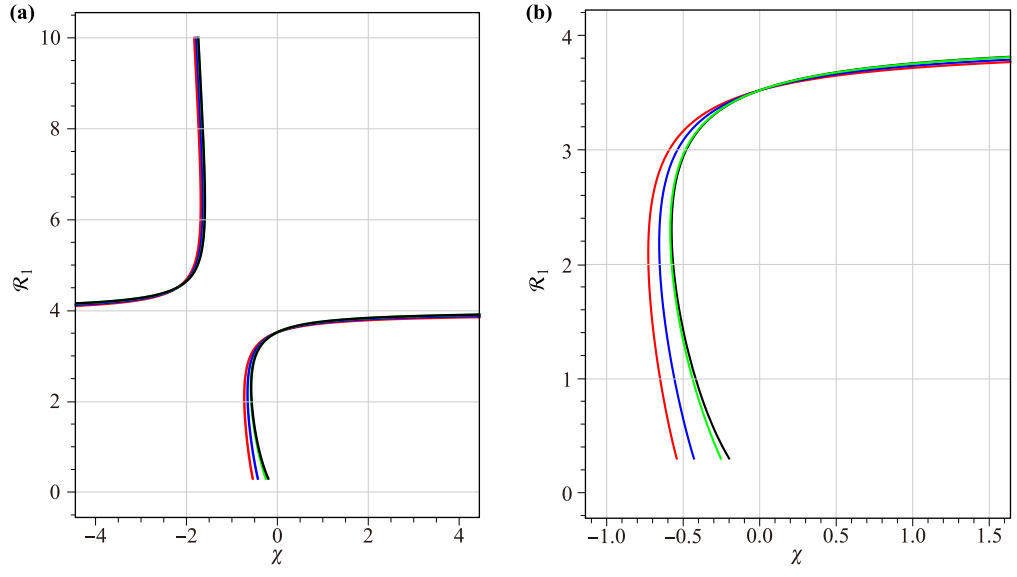

Fig. 2 **(a)** Value of the ratio $\mathcal{R}_1$ as a function of the parameter χ for $j = 1$ (red), 10 (blue), 100 (green), and ∞ (black). The right panel **(b)** is for a narrower range of χ to show differences between the curves in detail.

Table 1 Values of the parameter χ for various superconducting systems calculated from Eq. (15). The corresponding values of the ratio $\mathcal{R}_1$ and the critical temperature were taken from Refs. [14–19, 49–51].

Author	Material	T_c (K)	$\mathcal{R}_1$	χ
Bardeen *et al.* [14]	generic BCS		3.52	0
Ashcroft, Mermin [15]	Al	1.2	3.4	−0.197
	Cd	0.56	3.2	−0.381
	Hg	4.15	4.6	−2.052
	In	3.4	3.6	0.202
	Nb	9.26	3.8	1.454
	Pb	7.19	4.3	−2.869
	Sn	3.72	3.5	−0.040
	Ta	4.48	3.6	0.202
	Tl	2.39	3.6	0.202
	V	5.3	3.4	−0.197
	Zn	0.88	3.2	−0.381
Reber *et al.* [51]	strong-coupling SC		5	−1.755
	$Bi_2Sr_2CaCu_2O_8$	75	6.8	−1.599
	$Bi_2Sr_2CuO_6$	28	17.4	−2.075
	$Bi_2Sr_2CaCu_2O_8$ Ni-doped (1%)	80	7.83	−1.635
Ren *et al.* [50]	$Bi_2Sr_2CaCu_2O_{8+\delta}$	89	8.34	−1.658
Bianconi [49]	minimum value for doped cuprate perovskites of YBCO-type		0.35	−0.221

$\mathcal{R}_2(\chi)$ and $\mathcal{R}_4(\chi)$ from the formulas derived in the next sections.

3.2 Ratio $\mathcal{R}_2(\chi)$

Let us now derive the ratio $\mathcal{R}_2 \equiv \Delta C(T_c)/C_N(T_c)$, where $\Delta C(T_c) = C_S(T_c) - C_N(T_c)$, which defines the heat capacity jump between the superconducting phase and the normal phase at the transition temperature as a function of χ. To find the ratio, we need to consider Eqs. (5) and (6) at subcritical temperatures. Although any local fluctuation is precisely mapped onto $\varrho_j(x)$ for fixed j and χ, we have shown that, for values of $j > 100$ (corresponding to very narrow fluctuations), numerical and analytical results coincide with the case $j \to \infty$. Therefore, in further discussion, we consequently replace $\varrho_j(x)$ by $2\chi\delta(x)$.

3.2.1 *Subcritical temperature range*

For subcritical temperatures, i.e., for $T \lesssim T_c(\chi)$, in the case in which $\varrho(x)$ reduces to $2\chi\delta(x)$, Eq. (5) can be rewritten in the form

$$\frac{1}{g} = \nu_0 \left[\int_0^{x_p} \frac{\mathrm{d}x}{\sqrt{x^2+D^2}} \tanh\left(\sqrt{x^2+D^2}\right) + \chi \frac{\tanh D}{D} \right], \tag{16}$$

where now $x = \xi/(2T)$, $x_p = \xi_p/(2T)$, and $D = \Delta/(2T)$. Because, in the subcritical temperature range, the energy gap $\Delta(T,\chi)$ and hence $D(T,\chi) = \Delta(T,\chi)/(2T)$ are small, we derive our results using the second-order perturbation method. The right side of Eq. (16), after expanding it into a series including terms up to $D^4(T,\chi)$, assumes the form

$$\frac{1}{g} = \nu_0 \left[\ln\frac{\xi_p}{2T} + \chi - a\left(1+\frac{\chi}{3a}\right)\left(\frac{\Delta(T,\chi)}{2T}\right)^2 + b\left(1+\frac{2\chi}{15b}\right)\left(\frac{\Delta(T,\chi)}{2T}\right)^4 \right], \tag{17}$$

where

$$a = \frac{7\zeta(3)}{2\pi^2} = 0.426, \quad b = \frac{93\,\zeta(5)}{8\pi^4} = 0.124.$$

Taking into account the derived form of Eq. (17) for $T = T_c(\chi)$ and substituting it back into Eq. (17), we find

$$\Delta^2(T,\chi) = \frac{4T^2}{a\left(1+\frac{\chi}{3a}\right)} \left[-\ln\frac{T}{T_c(\chi)} + b\left(1+\frac{2\chi}{15b}\right)\left(\frac{\Delta(T,\chi)}{2T}\right)^4 \right]. \tag{18}$$

To solve Eq. (18) we use the perturbation method. Then, in the first and the second step of the method we obtain, respectively,

$$\Delta_I(T,\chi) = \frac{2T_c(\chi)}{\sqrt{a\left(1+\frac{\chi}{3a}\right)}}\sqrt{1-\frac{T}{T_c(\chi)}} = \frac{3.063T_c(\chi)}{\sqrt{1+0.782\chi}}\sqrt{1-\frac{T}{T_c(\chi)}} \tag{19}$$

and

$$\Delta_{II}(T,\chi) = \frac{2T_c(\chi)}{\sqrt{a\left(1+\frac{\chi}{3a}\right)}}\sqrt{1-\frac{T}{T_c(\chi)}}\left\{1-\left[\frac{3}{4}-\frac{b\left(1+\frac{2\chi}{15b}\right)}{2a^2\left(1+\frac{\chi}{3a}\right)^2}\right]\left(1-\frac{T}{T_c(\chi)}\right)\right\} = \frac{3.063T_c(\chi)}{\sqrt{1+0.782\chi}}\sqrt{1-\frac{T}{T_c(\chi)}}\left\{1-\left[\frac{3}{4}-\frac{0.341\,(1+1.077\chi)}{(1+0.782\chi)^2}\right]\left(1-\frac{T}{T_c(\chi)}\right)\right\}. \tag{20}$$

To have a complete set of the equations, let us find the free energy difference ΔF derived according to Eq. (6) in the second-order perturbation method. Employing Eqs. (17), (19), and (20), after some algebra, we obtain

$$\Delta F(T,\chi) = -\frac{\nu_0 T_c^2(\chi)}{a\left(1+\frac{\chi}{3a}\right)}\left(1-\frac{T}{T_c(\chi)}\right)^2\left\{1-\left[1-\frac{2b\left(1+\frac{2\chi}{15b}\right)}{3a^2\left(1+\frac{\chi}{3a}\right)^2}\right]\left(1-\frac{T}{T_c(\chi)}\right)\right\}$$
$$= -\frac{2.346\nu_0 T_c^2(\chi)}{1+0.782\chi}\left(1-\frac{T}{T_c(\chi)}\right)^2\left\{1-\left[1-\frac{0.454\,(1+1.077\chi)}{(1+0.782\chi)^2}\right]\left(1-\frac{T}{T_c(\chi)}\right)\right\}. \quad (21)$$

3.2.2 Specific heat difference

Employing standard thermodynamic relations, based on the free energy difference given by Eq. (21), we can find the reduced specific heat difference

$$\frac{\Delta C(T)}{C_N(T_c)} = \frac{6e^{\chi}}{\pi^2 a\left(1+\frac{\chi}{3a}\right)}\left\{1-\left[4-\frac{2b\left(1+\frac{2\chi}{15b}\right)}{a^2\left(1+\frac{\chi}{3a}\right)^2}\right]\left(1-\frac{T}{T_c(\chi)}\right)\right\}$$
$$= \frac{1.426e^{\chi}}{1+0.782\chi}\left\{1-\left[4-\frac{1.362\,(1+1.077\,\chi)}{(1+0.782\chi)^2}\right]\left(1-\frac{T}{T_c(\chi)}\right)\right\}, \quad (22)$$

where $C_N(T_c) = \frac{1}{3}\nu_0\pi^2 T_c$ must be constant and independent of χ. Therefore, $T_c \equiv T_c(0)$ and, to eliminate the ratio $T_c(\chi)/T_c(0)$ from Eq. (22), we have used Eq. (13) and replaced it with $T_c(\chi)/T_c(0) = e^{\chi}$. This expression can also be obtained from Eq. (19) or Eq. (20) by using formulas given in Refs. [13, 35]. The obtained expression allows us to find the characteristic ratio $\mathcal{R}_2 \equiv \Delta C(T_c)/C_N(T_c)$ quantifying the reduced specific heat jump at $T = T_c(\chi)$, which, eventually, can be found as

$$\mathcal{R}_2(\chi) = \frac{1.426e^{\chi}}{1+0.782\chi}. \quad (23)$$

Experimental data for the normalized heat capacity for CaAlSi and SrAlSi superconductors show that, in comparison to MgB_2 [23], the values of the heat capacity jump at the critical temperature can be above or below the value given by BCS theory. The ratio $\mathcal{R}_2(\chi)$ is a decreasing function of χ for $-0.576 < \chi < -0.279$ (dropping from 1.459 to 1.380) and becomes an increasing function for $\chi > -0.279$, below the BCS value of 1.426 obtained for $\chi = 0$.

Moreover, the ratio characterizing the slope of the line tangential to the reduced specific heat difference curve, which we denote as

$$\mathcal{R}_4 \equiv \frac{T_c}{C_N(T_c)}\left[\frac{d\Delta C(T)}{dT}\right]_{T=T_c},$$

is given by

$$\mathcal{R}_4(\chi) = \frac{1.426e^{\chi}}{1+0.782\chi}\left[4-\frac{1.362\,(1+1.077\chi)}{(1+0.782\chi)^2}\right] \quad (24)$$

and its dependence on the parameter χ is presented in Fig. 3.

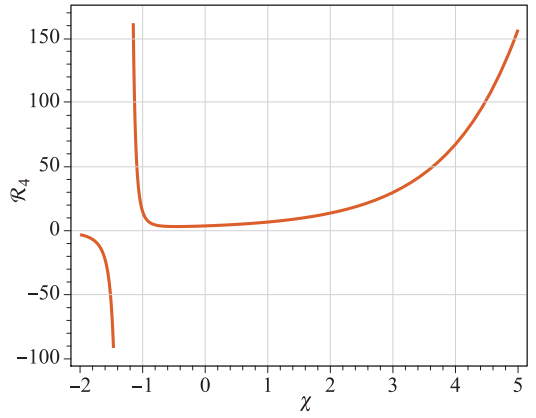

Fig. 3 Value of the ratio R_4 as a function of the parameter χ.

3.2.3 Additional relations and comments

Within the applied approximation $\varrho(x) \approx 2\chi\delta(x)$, Eq. (15) can be used to find χ as a function of $\mathcal{R}_1$. Then, by substituting it back into Eq. (23), we find $\mathcal{R}_2$ as a function $\mathcal{R}_1$ in the form

$$\mathcal{R}_2 = \frac{1.426(4-\mathcal{R}_1)}{4-\mathcal{R}_1+0.782\mathcal{R}_1\ln(\mathcal{R}_1/3.528)} \cdot \exp\left[\frac{\mathcal{R}_1\ln(\mathcal{R}_1/3.528)}{4-\mathcal{R}_1}\right]. \quad (25)$$

In Fig. 4 the graph of $\mathcal{R}_2$ versus $\mathcal{R}_1$ is plotted against experimental data for some standard low-T_c superconductors taken from Ref. [15]. The horizontal error bars denote the experimental uncertainty of $\mathcal{R}_1$, which is ± 0.1. The uncertainty of $\mathcal{R}_2$ is <10%.

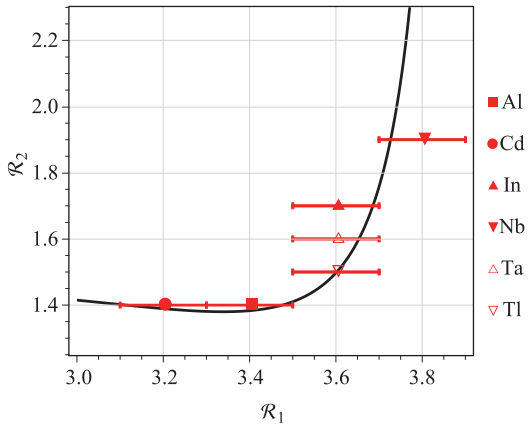

Fig. 4 Ratios $\mathcal{R}_1$ and $\mathcal{R}_2$ for some low-temperature superconducting materials. The experimental data for superconducting elements marked by the symbols explained in the legend are taken from Ref. [15].

Using Eq. (12), numerical values of $\mathcal{R}_1(\chi)$, and the formulas

$$\Delta(0,\chi) = \Delta(0,0)\exp\left[\frac{4\chi}{\mathcal{R}_1(\chi)}\right] \tag{26}$$

and

$$\Delta F(0,\chi) = -\frac{\nu_0}{4}\Delta^2(0,0)\exp\left[\frac{8\chi}{\mathcal{R}_1(\chi)}\right]\cdot\left[1+\frac{8\chi}{\mathcal{R}_1(\chi)}\right],$$

we evaluate $\Delta(0,\chi)$ and $\Delta F(0,\chi)$ numerically as functions χ (see Figs. 5 and 6).

Moreover, using Eqs. (13), (19), and (26), we can estimate the dependence of $\Delta(T,\chi)$ on χ for subcritical temperatures ($T \lesssim T_c(\chi)$). The first-order perturbation method yields

$$\Delta(T,\chi) = \Delta(0,0)\Phi(\chi)\sqrt{1-\frac{T}{T_c(\chi)}}, \tag{27}$$

where

$$\Phi(\chi) = \frac{2e^C e^{\chi}}{\pi\sqrt{a\left(1+\frac{\chi}{3a}\right)}} = 1.737\frac{e^{\chi}}{\sqrt{1+0.782\chi}}.$$

Therefore, the free energy difference is given by the formula

$$\Delta F(T,\chi) = -\frac{\nu_0}{4}\Delta^2(0,0)\Phi^2(\chi)\left(1-\frac{T}{T_c(\chi)}\right)^2 = -\frac{\nu_0}{4}\Delta^2(T,\chi)\left(1-\frac{T}{T_c(\chi)}\right).$$

The graph of $\Phi(\chi)$ is presented in Fig. 7.

Figure 8 shows the graph of the characteristic ratio $\mathcal{R}_1(\chi)$, found from Eq. (15), as a function of the parameter χ. The values of χ can be taken form the intervals $(-\infty,-1.59)$ and $(-0.576,\infty)$, and, although $\mathcal{R}_1(\chi)$ never achieves the limit value of 4, for large positive and negative values of χ it does tend to 4. However, for subcritical temperatures when $1+\frac{\chi}{3a} \le 0$, i.e., for $\chi \le -1.28$, the superconducting system under consideration becomes unstable, which implies that the interval $(-\infty,-1.59)$ must be excluded. However, because significant positive fluctuations in the density of states are responsible for enhancement of the critical temperature in high-T_c superconductors [3, 8, 39, 44], one can assume that χ can be chosen from a large part of the interval $(-0.576,\infty)$. More precisely, for negative values of χ from this interval, the critical temperature decreases

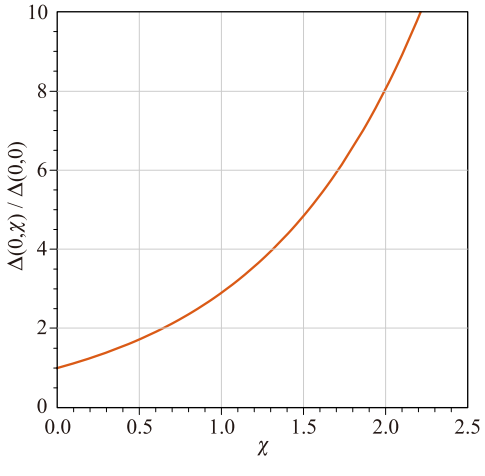

Fig. 5 Zero-temperature value of the energy gap as a function of the parameter χ.

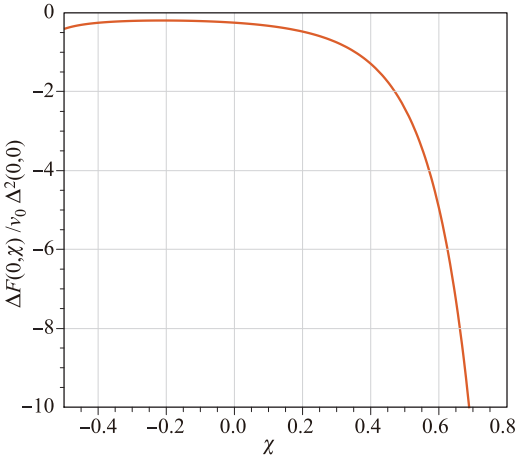

Fig. 6 Zero-temperature value of the free energy difference between the superconducting state and the normal state as a function of the parameter χ.

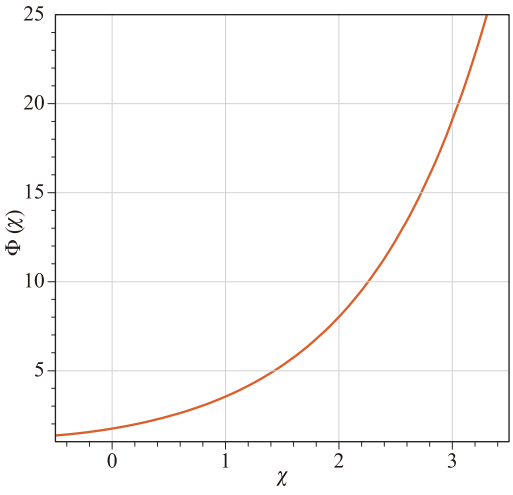

Fig. 7 Dependence of Φ on the parameter χ.

and $\mathcal{R}_1(\chi) < 3.52$, whereas for positive values the critical temperature increases and $\mathcal{R}_1(\chi) > 3.52$. Therefore, for all s-wave high-T_c superconductors, the value of $\mathcal{R}_1(\chi)$ should be close to 4. In particular, if χ varies from -0.576 to 6 then $\mathcal{R}_1(\chi)$ increases from 2.30 to 3.93.

In Table 2 we show that the experimental data $\mathcal{R}_1$ and $\mathcal{R}_2$ given in Ref. [15] for selected superconductors can be quite well reproduced within the present approach for a fixed value of χ. To illustrate versatility of the developed approach, we also include the values of $\mathcal{R}_4$ for these materials.

Of course, one should keep in mind limitations to the accuracy of experimental results, as well as simplifications applied in the discussed approach. Nevertheless, it is easy to note that, if the values of $\mathcal{R}_1$ for some superconductors are similar, then their ratios $\mathcal{R}_2$ coincide as well [14, 15], which is also confirmed within the present approach. The above results point to the fact that, for studies of low-T_c superconductors, χ should be taken from the interval $(-0.48, 2.0)$. Then $2.7 \leq \mathcal{R}_1 \leq 3.84$ and $1.46 \leq \mathcal{R}_2 \leq 4.11$. However, for high-$T_c$ superconductors when $\chi \gg 1$ and $T_c(\chi) \gg T_c(0)$, we should note that $\mathcal{R}_1(\chi) \approx 4$, whereas $\mathcal{R}_2(\chi)$ can achieve large values. Finally, it is worth adding a comment that some authors report estimated values of $\mathcal{R}_1$ far out of this interval for some superconductors of the new generation [23, 50, 51].

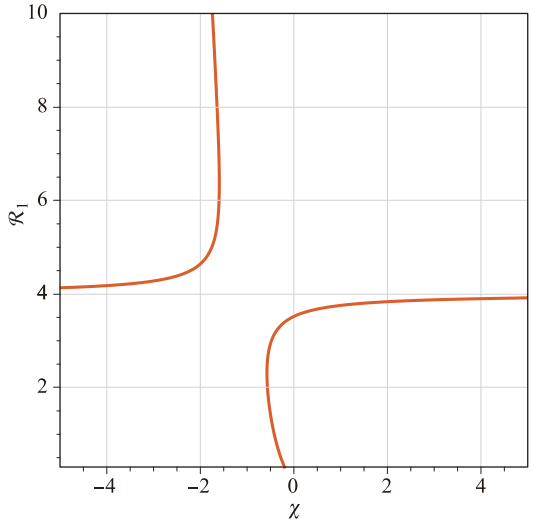

Fig. 8 Value of the ratio $\mathcal{R}_1$ as a function of the parameter χ in the limit $j \to \infty$.

Table 2 Comparison of experimental data of a few superconductors (SC) found within the established approach for a few values of the parameter χ.

SC	T_c (K)	$\mathcal{R}_1$	$\mathcal{R}_2$	χ	$\mathcal{R}_1(\chi)$	$\mathcal{R}_2(\chi)$	$\mathcal{R}_4$ (χ)
Al	1.29	3.3	1.4	−0.197	3.4	1.38	3.46
Cd	0.56	3.2	1.4	−0.381	3.2	1.39	3.29
Tl	2.39	3.6	1.5	0.202	3.6	1.51	4.16
Ta	4.48	3.6	1.6	0.339	3.64	1.58	4.49

4 Conclusions

In this paper, we have discussed the mathematical structure of the s-wave superconducting gap, the free energy, and the specific heat difference at $T = 0$ and in the subcritical temperature range using the method of successive approximations. Within the formalism, we have presented a systematic method for mapping between real superconducting systems and model systems characterized by a parameter χ. We have discussed a number of quantitative characteristics describing superconducting systems, both analytically and numerically, and have shown that the obtained theoretical results coincide with experimental data.

In the developed approach, we have taken into account a model form of the function $\varrho(x)$, modifying the density of states, which has so far been treated as constant in local intervals. In particular, we have shown that, if the function $\varrho(x)$ features a one-parameter narrow fluctuation (a peak) in the vicinity of the Fermi level, thermodynamic properties of simple (elementary) and composed superconductors differ significantly [7, 14–16, 19]. In particular, large positive values of the parameter χ give rise to remarkable enhancement of the critical temperature of high-T_c superconductors. The results obtained for the ratio $\mathcal{R}_1(\chi)$, relating the zero-temperature energy gap and the critical temperature, show that the value of the ratio for large positive values of the parameter χ should tend to ~ 4. Consequently, the pairing energy per one

quasiparticle at $T = 0$, i.e., $\Delta(0, \chi)/2$, must be equivalent to the decoupling energy, which appears when the temperature achieves the critical value of $T_c(\chi)$. Because the developed formalism is simplified and omits some interaction effects, the quantitative assessment presented in the paper may be improved by their inclusion. However, the overall contribution resulting from these extra effects would change the overall depiction only to a small degree (several per cent). What can significantly change the results is a more complicated form of the function $\rho(x)$, featuring several peaks located both on and off the Fermi level. The model can be extended in this direction to take into account the effects of high pressure.

The present approach could also be extended to include the effects of an external magnetic field. In particular, the zero-temperature critical magnetic field $H_c(0, \chi)$ could be derived, allowing one to evaluate another characteristic ratio $\mathcal{R}_3(\chi) \equiv H_c(0, \chi)/\sqrt{\nu_0}\Delta(0, \chi)$. For a system with a one-parameter narrow fluctuation in density of states, the results could then be compared with the data on $H_c(0)$ [16–19]. A standard method would take into account the magnetic field by including it in the equation for the free energy at $T = 0$ [13, 14, 19, 35].

Finally, let us also emphasize that, although the approach presented in this paper corresponds to the Van Hove scenario, it is obtained in a quite general manner by applying the more general conformal transformation method that includes the Van Hove scenario as its special case [3, 7, 8, 28, 35].

Acknowledgements This research was supported by Ministry of Science and Higher Education (Poland) in 2017–2018.

References

1. Y. Kamihara, T. Watanabe, M. Hirano, and H. Hosono, Iron-based layered superconductor La[$O_{1-x}F_x$]FeAs (x = 0.05–0.12) with T_c = 26 K, *J. Am. Chem. Soc.* 130(11), 3296 (2008)
2. H. Hosono and K. Kuroki, Iron-based superconductors: Current status of materials and pairing mechanism, *Physica C* 514, 399 (2015)
3. M. Krzyzosiak, R. Gonczarek, A. Gonczarek, and L. Jacak, Conformal Transformation Method in Studies of High-T_c Superconductors – Beyond the Van Hove Scenario in: Superconductivity and Superconducting Wires, Eds. D. Matteri and L. Futino, Nova Science Publishers, Hauppage, New York, 2010, Ch. 5
4. R. Gonczarek and M. Krzyzosiak, Model of Superconductivity in the Singular Fermi Liquid in: Progress in Superconductivity Research, Ed. O. A. Chang, Nova Science Publishers, Hauppage, New York, 2008, Ch. 6
5. R. Gonczarek and M. Krzyzosiak, Conformal transformation method and symmetry aspects of the group C_{4v} in a model of high-T_c superconductors with anisotropic gap, *Physica C* 426(431), 278 (2005)
6. R. Gonczarek, L. Jacak, M. Krzyzosiak, and A. Gonczarek, Competition mechanism between singlet and triplet superconductivity in the tight-binding model with anisotropic attractive potential, *Eur. Phys. J. B* 49(2), 171 (2006)
7. R. Gonczarek, M. Krzyzosiak, L. Jacak, and A. Gonczarek, Coexistence of spin-singlet s- and d-wave and spin-triplet p-wave order parameters in anisotropic superconductors, *phys. stat. sol. (b)* 244, 3559 (2007)
8. R. Gonczarek, M. Krzyzosiak, and A. Gonczarek, Islands of stability of the d-wave order parameter in s-wave anisotropic superconductors, *Eur. Phys. J. B* 61(3), 299 (2008)
9. D. Kasinathan, K. W. Lee, and W. E. Pickett, On heavy carbon doping of MgB_2, *Physica C* 424(3–4), 116 (2005)
10. J. Kortus, O. V. Dolgov, R. K. Kremer, and A. A. Golubov, Band filling and interband scattering effects in MgB_2: Carbon versus aluminum doping, *Phys. Rev. Lett.* 94(2), 027002 (2005)
11. W. S. Agrestini, C. Metallo, M. Filippi, L. Simonelli, G. Campi, C. Sanipoli, E. Liarokapis, S. De Negri, M. Giovannini, A. Saccone, A. Latini, and A. Bianconi, Substitution of Sc for Mg in MgB_2: Effects on transition temperature and Kohn anomaly, *Phys. Rev. B* 70(13), 134514 (2004)
12. H. Mori, T. Okano, M. Kamiya, M. Haemori, H. Suzuki, S. Tanaka, Y. Nishio, K. Kajita, and H. Moriyama, Bandwidth and band filling control in organic conductors, *Physica C* 357–360, 103 (2001)
13. M. Mulak and R. Gonczarek, Structures of thermodynamic functions for S-paired fermi systems in parametric equations approach, *Acta Phys. Pol. A* 89(5–6), 689 (1996)
14. A. L. Fetter and J. D. Walecka, Quantum Theory of Many-Particle Systems, McGraw-Hill Book Company, 1971, §51
15. N. W. Ashcroft and N. D. Mermin, Solid State Physics, Holt, Rinehart and Winston, 1976, Ch. 34 Superconductivity
16. C. Kittel, Introduction to Solid State Physics, John Wiley and Sons, Inc. NY, 1966, Ch. 11
17. J. Spałek, Introduction to Condensed Matter Physics, Wydawnictwo Naukowe PWN SA, Warszawa, 2015, Ch. 17
18. H. Ibach and H. Lüth, Solid State Physics. An Introduction to Principles of Material Science, Berlin Heidelberg: Springer-Verlag, 1995, Ch. 10.5
19. M. Cyrot and D. Pavuna, Introduction to Superconductivity and High-T_c Materials, World Scientific Publ. Co. (London, New Jersey, Singapore, Hong Kong, Bangalore, Beijing, 1992), Ch. 7.1

20. A. P. Durajski, R. Szczęśniak, and Y. Li, Non-BCS thermodynamic properties of H_2S superconductor, *Physica C* 515, 1 (2015)
21. A. P. Durajski and R. Szczęśniak, Estimation of the superconducting parameters for silane at high pressure, *Mod. Phys. Lett. B* 28(07), 1450052 (2014)
22. R. Szczęśniak, A. P. Durajski, M. W. Jarosik, Specific heat and thermodynamic critical field for calcium under the pressure at 120 GPa, *Mod. Phys. Lett. B* 26(08), 1250050 (2012)
23. B. Lorenz, J. Cmaidalka, R. L. Meng, and C. W. Chu, Thermodynamic properties and pressure effect on the superconductivity in CaAlSi and SrAlSi, *Phys. Rev. B* 68(1), 014512 (2003)
24. A. P. Durajski, Quantitative analysis of nonadiabatic effects in dense H_3S and PH_3 superconductors, *Sci. Rep.* 6(1), 38570 (2016)
25. A. Drozdov, M. I. Eremets, I. A. Troyan, V. Ksenofontov, and S. I. Shylin, Conventional superconductivity at 203 kelvin at high pressures in the sulfur hydride system, *Nature* 525(7567), 73 (2015)
26. M. Einaga, M. Sakata, T. Ishikawa, K. Shimizu, M. I. Eremets, A. P. Drozdov, I. A. Troyan, N. Hirao, and Y. Ohishi, Crystal structure of the superconducting phase of sulfur hydride, *Nat. Phys.* 12(9), 835 (2016)
27. Y. Li, J. Hao, H. Liu, Y. Li, and Y. Ma, The metallization and superconductivity of dense hydrogen sulfide, *J. Chem. Phys.* 140(17), 174712 (2014)
28. R. Gonczarek, M. Gładysiewicz, and M. Mulak, On possible formalism of anisotropic fermi liquid and BCS–type superconductivity, *Int. J. Mod. Phys. B* 15(05), 491 (2001)
29. F. C. Zhang and T. M. Rice, Effective Hamiltonian for the superconducting Cu oxides, *Phys. Rev. B* 37(7), 3759 (1988)
30. R. Szczęśniak and A. P. Durajski, The thermodynamic properties of the high-pressure superconducting state in the hydrogen-rich compounds, *Solid State Sci.* 25, 45 (2013)
31. R. Szczęśniak and A. P. Durajski, Superconducting state above the boiling point of liquid nitrogen in the GaH_3 compound, *Supercond. Sci. Technol.* 27(1), 015003 (2013)
32. D. Y. Xing, M. Liu, Y. G. Wang, and J. Dong, Analytic approach to the antiferromagnetic van Hove singularity model for high-T_c superconductors, *Phys. Rev. B* 60(13), 9775 (1999)
33. E. Pavarini, I. Dasgupta, T. Saha-Dasgupta, O. Jepsen, and O. K. Andersen, Band-structure trend in hole-doped cuprates and correlation with T_c max, *Phys. Rev. Lett.* 87(4), 047003 (2001)
34. O. K. Andersen, A. I. Liechtenstein, O. Jepsen, and F. Paulsen, LDA energy bands, low-energy hamiltonians, t', t'', $t_\wedge(k)$, and $J_\wedge$, *J. Phys. Chem. Solids* 56(12), 1573 (1995)
35. R. Gonczarek and M. Krzyzosiak, Some universal relations between the gap and thermodynamic functions plausible for various models of superconductors, *phys. stat. sol. (b)* 238, 29 (2003)
36. R. Szczęśniak, A. P. Durajski, and L. Herok, Theoretical description of the $SrPt_3P$ superconductor in the strong-coupling limit, *Phys. Scr.* 89(12), 125701 (2014)
37. R. Szczęśniak and A. P. Durajski, The Energy Gap in the $(Hg_{1-x}Sn_x)Ba_2Ca_2Cu_3O_{8+y}$ Superconductor, *Journal of Superconductivity and Novel Magnetism* 27(6), 1363 (2014)
38. R. Szczęśniak and A. P. Durajski, Thermodynamics of the superconducting state in calcium at 200 GPa, *Journal of Superconductivity and Novel Magnetism* 25(2), 399 (2012)
39. M. Krzyzosiak, R. Gonczarek, A. Gonczarek, and L. Jacak, Applications of the conformal transformation method in studies of composed superconducting systems, *Front. Phys.* 11(6), 117407 (2016)
40. R. Baquero, D. Quesada, and C. Trallero-Giner, BCS-universal ratios within the Van Hove scenario, *Physica C* 271(1–2), 122 (1996)
41. M. Mulak and R. Gonczarek, Discontinuous phase transitions in S-paired Fermi systems, *Acta Physica Polonica A* 92, 1177 (1997)
42. R. Gonczarek, M. Krzyzosiak, and M. Mulak, Valuation of characteristic ratios for high-T_c superconductors with anisotropic gap in the conformal transformation method, *J. Phys. A* 37(18), 4899 (2004)
43. R. Gonczarek, M. Gładysiewicz, and M. Mulak, Equilibrium states and thermodynamical properties of d-wave paired HTSC in the tight-binding model, *phys. stat. sol. (b)* 233, 351 (2002)
44. R. Gonczarek and M. Mulak, Enhancement of critical temperature of superconductors implied by the local fluctuation of EDOS, *Phys. Lett. A* 251(4), 262 (1999)
45. J. Bouvier and J. Bok, The gap symmetry and fluctuations in high T_c superconductors, Eds. J. Bok, G. Deutscher, D. Pavuna, and S. Wolf, Plenum Press, New York, 1998, p. 37
46. R. Baquero, D. Quesada, and C. Trallero-Giner, BCS-universal ratios within the Van Hove scenario, *Physica C* 271(1–2), 122 (1996)
47. R. Gonczarek, M. Krzyzosiak, A. Gonczarek, and L. Jacak, New classes of integrals inherent in the mathematical structure of extended equations describing superconducting systems, *Int. J. Mod. Phys. B* 29(17), 1550117 (2015)

48. R. Gonczarek, M. Krzyzosiak, A. Gonczarek, and L. Jacak, On new families of integrals in analytical studies of superconductors within the conformal transformation method, *Adv. Condens. Matter Phys.* 2015, 1 (2015)

49. A. Bianconi and M. Filippi, Feshbach Shape Resonances in Multiband high T_c Superconductors in: Symmetry and Heterogeneity in High Temperature Superconductors, Ed. A. Bianconi, NATO Science Series (II): Mathematics, Physics and Chemistry - Vol. 2014, Springer 2006, Ch. 1.2

50. J. K. Ren, X. B. Zhu, H. F. Yu, Y. Tian, H. F. Yang, C. Z. Gu, N. L. Wang, Y. F. Ren, and S. P. Zhao, Energy gaps in $Bi_2Sr_2CaCu_2O_{8+d}$ cuprate superconductors, *Sci. Rep.* 2(1), 248 (2012)

51. T. J. Reber, S. Parham, N. C. Plumb, Y. Cao, H. Li, Z. Sun, Q. Wang, H. Iwasawa, M. Arita, J. S. Wen, Z. J. Xu, G. D. Gu, Y. Yoshida, H. Eisaki, G. B. Arnold, and D. S. Dessau,Pairing, pair-breaking, and their roles in setting the T_c of cuprate high temperature superconductors, arXiv: 1508.06252v1 (2015)